Vascular Response of the Segments Adjacent to the Proximal and Distal Edges of the ABSORB Everolimus-Eluting Bioresorbable Vascular Scaffold: 6-Month and 1-Year Follow-Up Assessment

A Virtual Histology Intravascular Ultrasound Study From the First-in-Man ABSORB Cohort B Trial

Bill D. Gogas, MD,* Patrick W. Serruys, MD, PHD,* Roberto Diletti, MD,*
Vasim Farooq, MBCHB,* Salvatore Brugaletta, MD,* Maria D. Radu, MD,*
Jung Ho Heo, MD,* Yoshinobu Onuma, MD,* Robert-Jan M. van Geuns, MD, PHD,*
Evelyn Regar, MD, PHD,* Bernard De Bruyne, MD, PHD,† Bernard Chevalier, MD,‡
Leif Thuesen, MD,§ Pieter C. Smits, MD, PHD,‖ Dariusz Dudek, MD,¶
Jacques Koolen, MD, PHD,# Stefan Windecker, MD,** Robert Whitbourn, MD,††
Karine Miquel-Hebert, PHD,‡‡ Cecile Dorange, MSC,‡‡ Richard Rapoza, PHD,§§
Hector M. Garcia-Garcia, MD, MSC, PHD,‖‖ Dougal McClean, MD,¶¶
John A. Ormiston, MBCHB, PHD##

*Rotterdam and Eindhoven, the Netherlands; Aalst and Diegem, Belgium; Massy, France;
Aarhus, Denmark; Krakow, Poland; Bern, Switzerland; Fitzroy, Australia; Santa Clara,
California; and Christchurch and Auckland, New Zealand*

Objectives This study sought to investigate in vivo the vascular response at the proximal and distal edges of the second-generation ABSORB everolimus-eluting bioresorbable vascular scaffold (BVS).

Background The edge vascular response after implantation of the BVS has not been previously investigated.

Methods The ABSORB Cohort B trial enrolled 101 patients and was divided into B_1 (n = 45) and B_2 (n = 56) subgroups. The adjacent (5-mm) proximal and distal vessel segments to the implanted ABSORB BVS were investigated at either 6 months (B_1) or 1 year (B_2) with virtual histology intravascular ultrasound (VH-IVUS) imaging.

Results At the 5-mm proximal edge, the only significant change was modest constrictive remodeling at 6 months (Δ vessel cross-sectional area: -1.80% [-3.18; 1.30], $p < 0.05$), with a tendency to regress at 1 year (Δ vessel cross-sectional area: -1.53% [-7.74; 2.48], $p = 0.06$). The relative change of the fibrotic and fibrofatty (FF) tissue areas at this segment were not statistically significant at either time point. At the 5-mm distal edge, a significant increase in the FF tissue of 43.32% [-19.90; 244.28], ($p < 0.05$) 1-year post-implantation was evident. The changes in dense calcium need to be interpreted with caution since the polymeric struts are detected as "pseudo" dense calcium structures with the VH-IVUS imaging modality.

Conclusions The vascular response up to 1 year after implantation of the ABSORB BVS demonstrated some degree of proximal edge constrictive remodeling and distal edge increase in FF tissue resulting in nonsignificant plaque progression with adaptive expansive remodeling. This morphological and tissue composition behavior appears to not significantly differ from the behavior of metallic drug-eluting stents at the same observational time points. (J Am Coll Cardiol Intv 2012;5:656–65) © 2012 by the American College of Cardiology Foundation

The vascular response at the stent edges has been evaluated with first-generation drug-eluting stents and appears to be dependent on the implanted device and the periprocedural induced vascular trauma because of the geographic miss (GM) phenomenon (1). The initial trial with the sirolimus-eluting stent—RAVEL (RAndomized study with the sirolimus-eluting VElocity balloon-expandable stent in the treatment of patients with de novo native coronary artery Lesions)—demonstrated no significant edge effect, presumably due to the exceptional stent/lesion ratio of 2:1, due to the sole availability of stent length (18 mm). A significant proximal edge lumen loss was, however, observed in the SIRIUS (Sirolimus-Coated Bx Velocity Balloon-Expandable Stent in the Treatment of De Novo Native Coronary Artery Lesions) trial, which evaluated the same stent platform as in RAVEL, but with several stent lengths and diameters of the device in a more complex population. In the first-in-man TAXUS I trial, no edge effect was demonstrated with the use of the slow-release polymer formulation of the paclitaxel-eluting stent; conversely, in the TAXUS II trial, the slow-release and moderate-release polymer formulations of the paclitaxel-eluting stent resulted in an edge lumen area loss (-0.54 ± 2.1 mm^2 and -0.88 ± 1.9 mm^2, respectively) at both the proximal and distal stent edges (2,3). In the BETAX (BEside TAXus) trial, using the Taxus Express drug-eluting stent, significant tissue compositional changes were observed, mainly due to an increase in the fibrofatty (FF) tissue component causing expansive remodeling at both stent edges (4).

Pre-clinical research has demonstrated that the tissue response after stent implantation is exclusively composed of proteoglycan-rich smooth muscle cells and fibrolipidic areas rich in collagen and reticular fibers (5). This iatrogenic entity of neointimal hyperplasia has been demonstrated to be usually focal and most commonly located at the proximal stent edge (6). The advent of scaffolds with bioresorbable properties and differing biological behavior compared with the currently used metallic devices, has prompted the re-evaluation of the edge vascular response using sound-based imaging modalities with tissue characterization properties. Such a modality is the virtual histology intravascular ultrasound (VH-IVUS), which allows for the evaluation of the vascular geometric changes and assessment of the atheromatous plaque progression/regression.

The purpose of this study is to investigate the edge effect after the implantation of the ABSORB bioresorbable vascular scaffold (BVS) in the assessment of the geometric and compositional changes of the segments adjacent to the 5-mm proximal and distal edges of the scaffolded vessel, in a population investigated at either 6 months or 1 year post scaffold implantation.

Methods

Study design and population. The ABSORB Cohort B trial is a multicenter, ongoing, single-arm prospective, open-label trial assessing the safety and performance of the second-generation ABSORB BVS in the treatment of patients with a maximum of 2 de novo native coronary artery lesions. In total, 101 patients were enrolled and subdivided into 2 subgroups—Cohort B_1 (n = 45) and Cohort B_2 (n = 56)—according to the predefined study design. Both groups underwent invasive follow-up, Cohort B_1 at 6 months and Cohort B_2 at 1 year. Cohort B_1 is currently undergoing a second VH-IVUS imaging of the scaffold edges at 2 -years and Cohort B_2 will undergo the final VH-IVUS imaging evaluation at 3 years (Fig. 1).
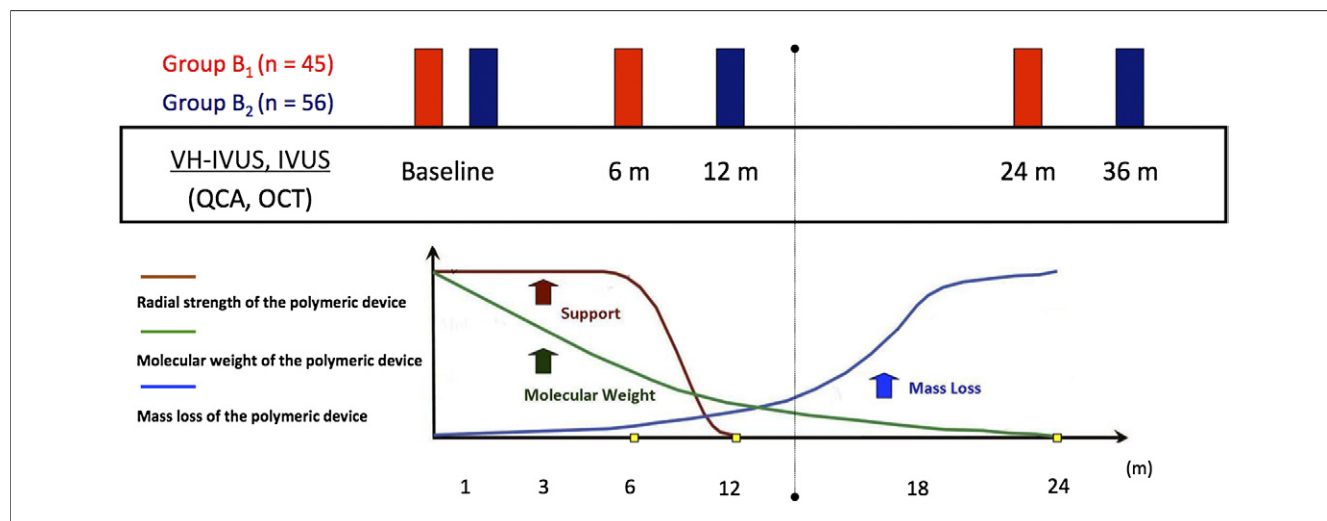
In the present study, patients over the age of 18 years, who had either stable or unstable angina pectoris or silent ischemia, were suitable for inclusion. All treated lesions were de novo lesions in a native coronary artery with a maximum diameter of 3.0 mm, a length of <14 mm, a percent diameter stenosis ≥50% and <100%, and a Thrombolysis In Myocardial Infarction (TIMI) flow grade of ≥1. Major exclusion criteria were patients presenting with an acute myocardial infarction or unstable arrhythmias, or patients who had a left ventricular ejection fraction <30%, restenotic lesions, lesions located in the left main coronary artery, lesions involving an epicardial side branch ≥2 mm in diameter by visual assessment, and the presence of thrombus or another clinically significant stenosis in the target vessel.

Abbreviations and Acronyms

CSA = cross-sectional area

DC = dense calcium

FF = fibrofatty

GM = geographic miss

NC = necrotic core

VH-IVUS = virtual histology intravascular ultrasound

WSS = wall shear stress

Figure 1. ABSORB Cohort B Study Design

The study design of the ABSORB Cohort B trial with the respective biological behavior of the ABSORB bioresorbable vascular scaffold, at the different time frames that virtual histology intravascular ultrasound (VH-IVUS) imaging was performed **(yellow points)**. OCT = optical coherence tomography; QCA = quantitative coronary angiography.

The ethics committee at each participating institution approved the protocol, and each patient gave written informed consent before inclusion.

Treatment device. The ABSORB BVS (Abbott Vascular, Santa Clara, California) is a balloon-expandable device consisting of a polymer backbone of poly-L-lactide coated with a thin layer of a 1:1 mixture of poly-D,L-lactide. The polymer controls the release of the antiproliferative drug everolimus, and forms an amorphous drug-eluting coating matrix that contains 100 μg of everolimus/cm^2 of scaffold. According to

Table 1. Baseline Clinical and Lesion Characteristics

	6 Months		1 Year	
	Proximal Edge (n = 23)	Distal Edge (n = 18)	Proximal Edge (n = 24)	Distal Edge (n = 29)
Age, yrs	62.41 ± 9.86	64.70 ± 9.83	59.21 ± 7.72	60.20 ± 7.72
Male	14 (61%)	12 (67%)	15 (63%)	20 (69.0%)
Current smoking	3 (13.0%)	1 (6%)	5 (21%)	2 (7%)
Diabetes	5 (22%)	3 (17%)	7 (29%)	6 (21%)
Hypertension	16 (70%)	13 (72%)	17 (74%)	19 (68%)
Hypercholesterolemia	22 (96%)	18 (100%)	18 (75%)	22 (76%)
Prior myocardial infarction	8 (35%)	7 (39%)	5 (21%)	3 (11%)
Unstable angina	3 (13%)	3 (17%)	4 (17%)	6 (21%)
Stable angina	16 (70%)	14 (78%)	14 (58%)	17 (59%)
Treated vessel				
Right coronary artery	9 (39%)	7 (39%)	9 (36%)	8 (27%)
Left anterior descending artery	6 (26%)	6 (33%)	10 (40%)	16 (53%)
Left circumflex artery	7 (30%)	4 (22%)	6 (24%)	6 (20%)
ACC/AHA lesion class:				
Type A	1 (4%)	1 (5%)	0 (0%)	0 (0%)
Type B1	10 (44%)	9 (50%)	17 (71%)	22 (73%)
Type B2	11 (48%)	8 (44%)	6 (25%)	7 (23%)
Type C	1 (4%)	0 (0%)	1 (4%)	1 (3%)
RVD before intervention, mm	2.56 ± 0.43	2.78 ± 0.45	2.61 ± 0.33	2.50 ± 0.28

Values are mean ± SD or n (%).
ACC/AHA = American College of Cardiology/American Heart Association; RVD = reference vessel diameter.

Table 2. Summary of the % Changes of the Entire 5-mm Segment, at the Proximal and Distal Edges, Regarding Geometric and Plaque Composition Parameters 6 Months and 1 Year Following Implantation of the ABSORB BVS

	Vessel CSA (mm^2)	Lumen CSA (mm^2)	Plaque CSA (mm^2)
Proximal edge segment, (%) change			
6 months (n = 23)	−1.8 [−3.18; 1.30]	−4.1 [−11.61; 8.79]	−4.04 [−10.65; 11.05]
p value	**<0.05**	NS	NS
1 year (n = 25)	−1.53 [−7.74; 2.48]	−5.32 [−12.36; 4.24]	−2.03 [−8.39; 7.76]
p value	NS	NS	NS
Distal edge segment, (%) change			
6 months (n = 18)	−0.59 [−3.74; 7.09]	−0.32 [−7.71; 7.20]	7 [−11.97; 18.36]
p value	NS	NS	NS
1 year (n = 30)	3.45 [−2.08; 6.91]	0.95 [−7.56; 7.48]	5.73 [−6.49; 25.47]
p value	NS	NS	NS

	Dense Calcium (mm^2)	Fibrous (mm^2)	Fibrofatty (mm^2)	Necrotic Core (mm^2)
Proximal edge segment, (%) change				
6 months (n = 23)	12.02 [−31.62; 47.50]	4.44 [−16.83; 67.23]	10.3 [−46.38; 134.69]	24.14 [−22.32; 76.76]
p value	NS	NS	NS	NS
1 year (n = 25)	−7.91 [−42.19; 17.26]	−2.58 [−20.03; 11.86]	−9 [−36.77; 87.41]	−4.35 [−31.23; 30.40]
p value	NS	NS	NS	NS
Distal edge segment, (%) change				
6 months (n = 18)	44.09 [22.81; 159.23]	4.07 [−18.83; 107.39]	8.21 [−37.77; 91.48]	23.59 [−19.89; 74.33]
p value	**<0.05**	NS	NS	NS
1 year (n = 30)	−20.57 [−50.22; 54.11]	18.87 [−11.14; 108.93]	43.32 [−19.90; 244.28]	−6.25 [−44.20; 81.94]
p value	NS	NS	**<0.05**	NS

p values in **bold** are statistically significant.
BVS = bioresorbable vascular scaffold; CSA = cross-sectional area; NS = not significant.

bench studies, the ABSORB BVS device has shown a dynamic biological behavior at 6 months, 1 year, and 2 years, at which time the complete bioresorption of the polymer backbone is expected (7).

At 6 months, a gradual and steep loss of the device radial strength in parallel to the continuous decrease of the device molecular weight is observed because of the depolymerization and hydrolysis after implantation. The molecular weight of the polymeric platform continues to decrease until 1 year, when the radial strength is completely eliminated, and the device represents a passive structure without any supportive vascular properties. At 2 years, the ABSORB

Table 3. Summary of the Proximal and Distal Edge Changes at 6 Months and 1 Year After Implantation of the ABSORB BVS

	Time After the Imaging Procedure					
	Vessel CSA (mm^2)	Lumen CSA (mm^2)	Plaque CSA (mm^2)	Vessel CSA (mm^2)	Lumen CSA (mm^2)	Plaque CSA (mm^2)
Proximal Edge	6 Months (n = 23)			1 Year (n = 25)		
Baseline	13.2 [10.81; 15.90]	7.15 [5.80; 8.65]	5.88 [4.22; 7.08]	13.89 [12.55; 17.24]	7.25 [6.44; 8.40]	7.02 [5.52; 7.80]
Follow-up	13.38 [10.26; 15.39]	7.15 [5.60; 8.41]	5.49 [3.86; 7.25]	13.71 [12.22; 16.11]	7 [6.14; 8.30]	7.08 [5.36; 8.38]
Median absolute difference	−0.25 [−0.54; 0.18]	−0.27 [−0.78; 0.67]	−0.25 [−0.63; 0.60]	−0.19 [−1.06; 0.33]	−0.35 [−0.77; 0.25]	−0.15 [−0.59; 0.37]
p value	**<0.05**	NS	NS	NS	NS	NS
Distal Edge	6 Months (n = 18)			1 Year (n = 30)		
Baseline	12.79 [10.17; 16.38]	7.27 [5.62; 7.90]	7.02 [4.15; 7.89]	10.28 [9.13; 13.46]	6.7 [5.63; 7.80]	4.47 [2.29; 5.61]
Follow-up	13.87 [10.42; 16.15]	6.85 [6.11; 8.44]	6.07 [4.90; 8.40]	10.49 [9.88; 13.33]	6.76 [5.56; 7.78]	4.46 [3.20; 6.61]
Median absolute difference	−0.07 [−0.51; 1.00]	−0.03 [−0.55; 0.58]	0.35 [−0.82; 0.97]	0.4 [−0.26; 0.63]	0.09 [−0.49; 0.43]	0.27 [−0.27; 0.97]
p value	NS	NS	NS	NS	NS	NS

Values are medians (interquartile ranges). Analysis was performed at the lesion level.
Abbreviations as in Table 2.

Table 4. Summary of the Tissue Composition Changes at the Proximal and Distal Edges, 1 Year After Implantation of the ABSORB BVS

	Dense Calcium (mm^2)	Dense Calcium (%)	Fibrous (mm^2)
Proximal edge segment (n = 25)			
Baseline	0.48 [0.24; 0.76]	12.55 [7.02; 20.20]	1.95 [1.01; 2.69]
1-year follow-up	0.33 [0.24; 0.54]	11.97 [8.31; 17.94]	2.02 [1.37; 2.41]
Median absolute difference	−0.02 [−0.20; 0.09]	−0.72 [−3.70; 4.65]	−0.04 [−0.33; 0.20]
p value	NS	NS	NS
Distal edge segment (n = 30)			
Baseline	0.18 [0.08; 0.57]	15.87 [10.17; 35.30]	0.91 [0.08; 1.61]
1-year follow-up	0.19 [0.08; 0.31]	10.5 [6.93; 17.07]	0.9 [0.28; 1.52]
Median absolute difference	−0.02 [−0.20; 0.07]	−4.22 [−12.18; 1.35]	0.09 [−0.07; 0.22]
p value	NS	**<0.05**	NS

p values in **bold** are statistically significant.

Abbreviations as in Table 3.

BVS is considered fully resorbed, having been metabolized into CO_2 and H_2O through the Krebs cycle (Fig. 1). This dynamic behavior of the polymeric device at the above-mentioned time points prompts the in vivo evaluation of the vascular response at the scaffold edges with VH-IVUS imaging in parallel to its evolving biological behavior (8).

Treatment procedure. Lesions were treated with routine interventional techniques that included mandatory pre-dilation with a balloon shorter and 0.5 mm smaller in diameter than the study device. The ABSORB BVS was implanted at a pressure not exceeding the rated burst pressure (16 atm). Post-dilation with a balloon shorter than the implanted device was allowed at the discretion of the operator, as was bailout treatment.

Quantitative IVUS and VH-IVUS analysis. Geometric parameters in the complete 5-mm proximal and distal segments derived from the grayscale IVUS and VH-IVUS acquisition were analyzed in each separate frame—that is, vessel area, lumen area, plaque area, and tissue composition parameters—as absolute values. Furthermore, percentages were assessed for each cross section in the same region of interest. Both the proximal and distal vessel segments were further divided into 1-mm subsegments, numbered from 1 (adjacent to the scaffold) to 5, and underwent similar imaging evaluation as for the complete segment.

The tissue compositional analysis was obtained with a phased-array 20-MHz intravascular ultrasound catheter (Eagle Eye, Volcano Corporation, Rancho Cordova, California) after intracoronary administration of 100 to 200 μg of nitroglycerin, using automated pullback at 0.5 mm/second (30 frames/s). The raw radiofrequency data were capture gated to the R-wave. The main principle of the VH-IVUS imaging technique is that both the envelope amplitude of the reflected radiofrequency signals, as undertaken with standard grayscale IVUS analyses, and the underlying frequency content is used to analyze the tissue components present in coronary plaques. The combined information is subsequently processed using autoregressive

models and thereafter categorized into a classification tree that determines the 4 basic plaque tissue components: 1) fibrous tissue—dark green; 2) FF—light green; 3) necrotic core (NC)—red; and 4) dense calcium (DC)—white (9). All VH-IVUS analyses were performed offline using the pcVH 2.1 software (Volcano Corporation) by an independent clinical research organization (Cardialysis, Rotterdam, the Netherlands). At 6 months (Cohort B$_1$, n = 45), 23 proximal and 18 distal edge segments were suitable for analysis with grayscale IVUS and VH-IVUS imaging. At 1 year (Cohort B$_2$, n = 56), 25 proximal and 30 distal edge segments were analyzable. The reasons for the reduced number of our final tested samples were: 1) the dropout of patients at follow-up (the attrition rate of the ABSORB Cohort B trial was ~20%) and exclusion of the unpaired samples from our final data; and 2) exclusion of cases, according to the standard operational procedure of the independent core laboratory (Cardialysis), with side-branch outgrowth of >90° at the side of the scaffold edge that did not allow the analysis of the complete 5-mm segment and vessel wall out of the field of the view.

Statistical analysis. Discrete variables are presented as counts and percentages. Continuous variables are presented as medians and interquartile ranges. Comparison between baseline and follow-up was performed using the Wilcoxon signed rank test. Changes (differences) for each measurement were calculated as follow-up minus post-procedure values. Percent changes (differences) for each variable were calculated as follow-up post-procedure/post-procedure ×100%. A p value <0.05 was considered statistically significant. Data analyses were performed with SAS version 9.1 software (SAS Institute, Cary, North Carolina).

Results

The baseline clinical and lesion characteristics of the patients are demonstrated in Table 1. The percent (%) changes

Table 4. Continued

Fibrous (%)	Fibrofatty (mm^2)	Fibrofatty (%)	Necrotic Core (mm^2)	Necrotic Core (%)
55.08 [46.10; 63.52]	0.26 [0.11; 0.45]	7.34 [4.99; 10.36]	0.85 [0.40; 1.28]	19.63 [17.16; 29.81]
53.62 [48.56; 59.95]	0.28 [0.09; 0.38]	8 [4.46; 11.39]	0.64 [0.42; 1.01]	20.49 [15.11; 29.02]
−0.1 [−4.67; 5.71]	−0.01 [−0.10; 0.19]	0.03 [−3.08; 3.42]	−0.06 [−0.32; 0.23]	−2.05 [−5.58; 5.65]
NS	NS	NS	NS	NS
54.72 [35.05; 62.19]	0.06 [0.01; 0.17]	4.7 [2.49; 7.87]	0.4 [0.04; 0.72]	21.96 [17.58; 28.00]
57.75 [51.27; 62.42]	0.1 [0.03; 0.28]	8.1 [4.23; 12.54]	0.3 [0.09; 0.64]	18.75 [14.65; 24.88]
1.83 [−4.36; 14.58]	0.02 [0.00; 0.09]	2.24 [0.48; 8.69]	−0.01 [−0.33; 0.09]	−2.82 [−7.26; 4.22]
NS	<0.05	<0.05	NS	NS

(median [interquartile range]) of the vessel cross-sectional area (CSA), lumen CSA, and plaque CSA at the 5-mm proximal edge segment were at 6 months: −1.80% [−3.18; 1.30], ($p < 0.05$), −4.10% [−11.61; 8.79], ($p = 0.22$), and −4.04% [−10.65; 11.05] ($p = 0.55$); and at 1 year: −1.53% [−7.74; 2.48], ($p = 0.06$), −5.32% [−12.36; 4.24], ($p = 0.07$), and −2.03% [−8.39; 7.76], ($p = 0.72$), respectively. The % changes of the vessel CSA, lumen CSA, and plaque CSA at the 5-mm distal edge segment were at 6 months: −0.59% [−3.74; 7.09], ($p = 0.71$), −0.32% [−7.71; 7.20],

($p = 0.97$), and 7.0% [−11.97; 18.36], ($p = 0.50$); and at 1 year: 3.45% [−2.08; 6.91], ($p = 0.07$), 0.95% [−7.56; 7.48], ($p = 0.77$), and 5.73% [−6.49; 25.47], ($p = 0.09$), respectively (Table 2). The absolute geometric and tissue composition changes and the subsegmental analysis at 1 year are tabulated in (Tables 3 and 4) and illustrated in Figs. 2, 3, and 4.

The absolute tissue compositional changes at 6 months at both edges and the subsegmental analysis at the same time point are tabulated and illustrated in the Online Appendix.
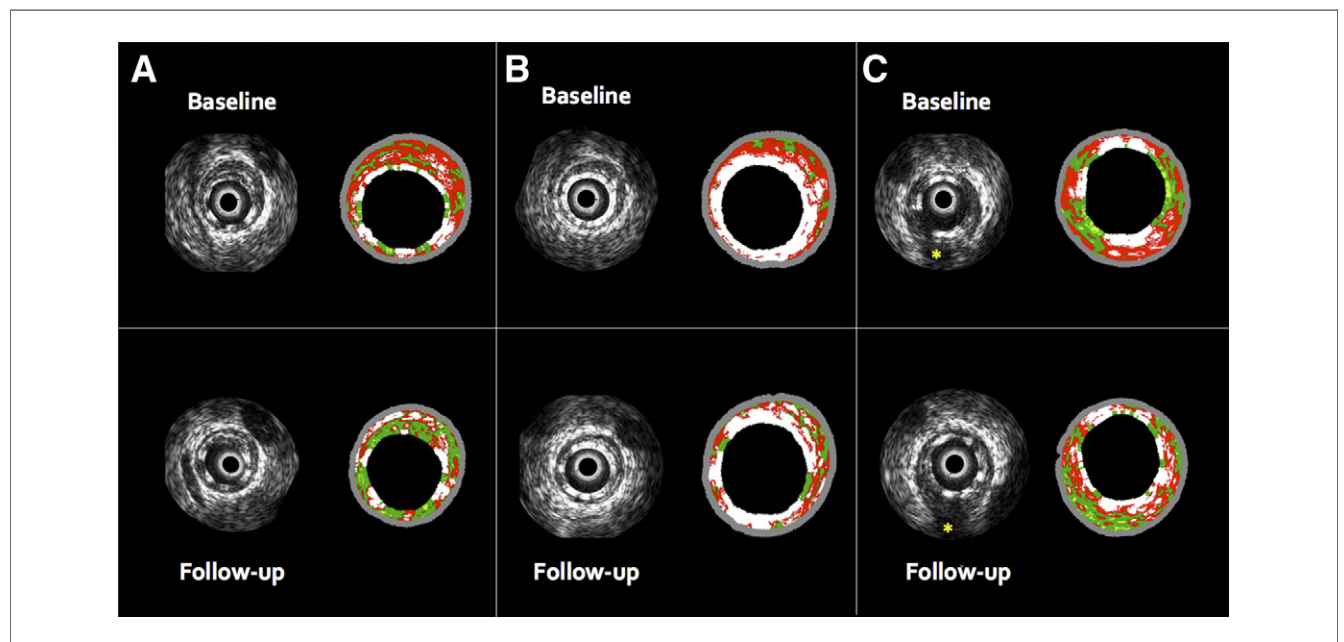
Figure 2. Grayscale IVUS and Corresponding VH-IVUS Still Frames at 1-Year After Implantation of the ABSORB BVS

(A) Distal edge segment. At this segment a significant increase of the fibrofatty (FF) tissue was observed. VH-IVUS demonstrates at this frame a change in FF tissue area from 0.07 to 0.14 mm^2. Dense calcium (DC) and necrotic core tissue components changed from 2.39 mm^2 and 3.7 mm^2 to 2.07 mm^2 and 1.8 mm^2, respectively, as a consequence of the bioresorption process. (B) Scaffolded segment. The polymeric struts of the ABSORB BVS are detected as "pseudo" DC surrounded by a red, halo. (C) Proximal edge segment. At this segment some degree of proximal edge constrictive vascular remodeling was observed. Grayscale IVUS shows for this frame a change in the lumen area from 9.4 mm^2 to 8.4 mm^2 (The external elastic membrane has been extrapolated at the side of the side branch, [yellow asterisk]).
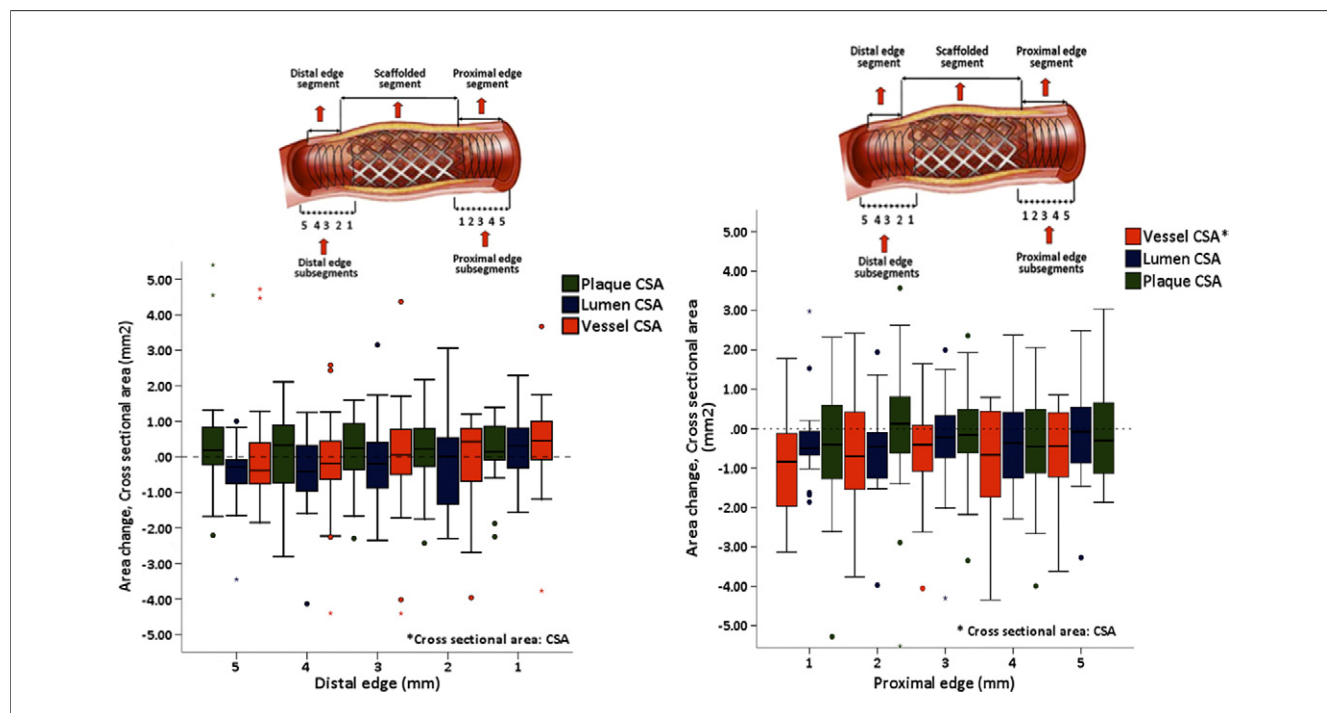
Figure 3. Subsegmental Analysis of the Geometric Changes at the Proximal and Distal Edges After Implantation of the ABSORB BVS

The analysis, per mm of the subsegments, was performed at 1-year follow-up. BVS = bioresorbable vascular scaffold.

Discussion

The main findings of this study at the time point of 1-year post-implantation of the ABSORB BVS are as follows. Constrictive vascular remodeling at the proximal edge was evident without significant changes in tissue composition parameters. At the distal edge, tissue composition changes were evident with a significant increase in the FF tissue resulting in nonsignificant plaque progression and adaptive expansive remodeling (Fig. 2).

The edge effects following the implantation of either a metallic or a polymeric device have common etiological mechanisms, namely: 1) periprocedural or iatrogenic technical issues affecting predominantly geometric parameters (1–11); 2) tissue composition characteristics of the lesion (12); and 3) local wall shear stress (WSS) conditions (13–15).

The GM phenomenon, associated with sirolimus-eluting stent implantation, was investigated in the STLLR (Stent Deployment Techniques on Clinical Outcomes of Patients Treated With the Cypher Stent) study and was reported to occur in nearly two-thirds (66.5%) of the study group; almost one-half of the patients (47.6%) experienced longitudinal GM, over one-third (35.2%) axial GM, and 16.5%, a combination of the 2 (1,10). Hoffmann et al. (10) demonstrated within the E-SIRIUS (European, multicenter, randomized, double blind trial of the SIRolImUS-coated Bx-Velocity stent in the treatment of patients with de novo coronary artery lesions)-IVUS substudy versus the SIRIUS-US (US, multicenter, randomized, double blind trial of the SIRolImUS-coated Bx-Velocity stent in the treatment of patients with de novo coronary artery lesions) trial, that both axial and longitudinal GM were reduced (from 5.9% to 2.1%) when periprocedural implantation parameters were taken into account, such as conservative pre-dilation, less forceful stent implantation (~16 atm), and selective post-dilation with balloons shorter than the stent.

Despite multiple technical guidelines regarding the ABSORB BVS delivery system to minimize the axial (burst pressure: 16 atm) and longitudinal (balloon shorter and 0.5 mm smaller than the implanted device) GM phenomena, a significant proximal edge constrictive response was demonstrated at 6 months, whereas at 1 year, the constrictive remodeling was only observed in the following proximal subsegments, starting from the scaffold edge (subsegment 1: Δ −0.96 mm^2, (p < 0.05); subsegment 2: Δ −0.71 mm^2, (p < 0.05); and subsegment 4: Δ −0.57(p < 0.05) (Figs. 3 and 4).

The changes in WSS distribution adjacent to the stent edges post device implantation appear to follow alterations in vessel curvature and angulation, and have been reported to result in step-up regions of low shear stress, prone to neointimal growth (13–15).

Metallic devices have a more accentuated effect on vessel curvature and angulation compared to the ABSORB BVS; however, despite the clinical benefits associated with better
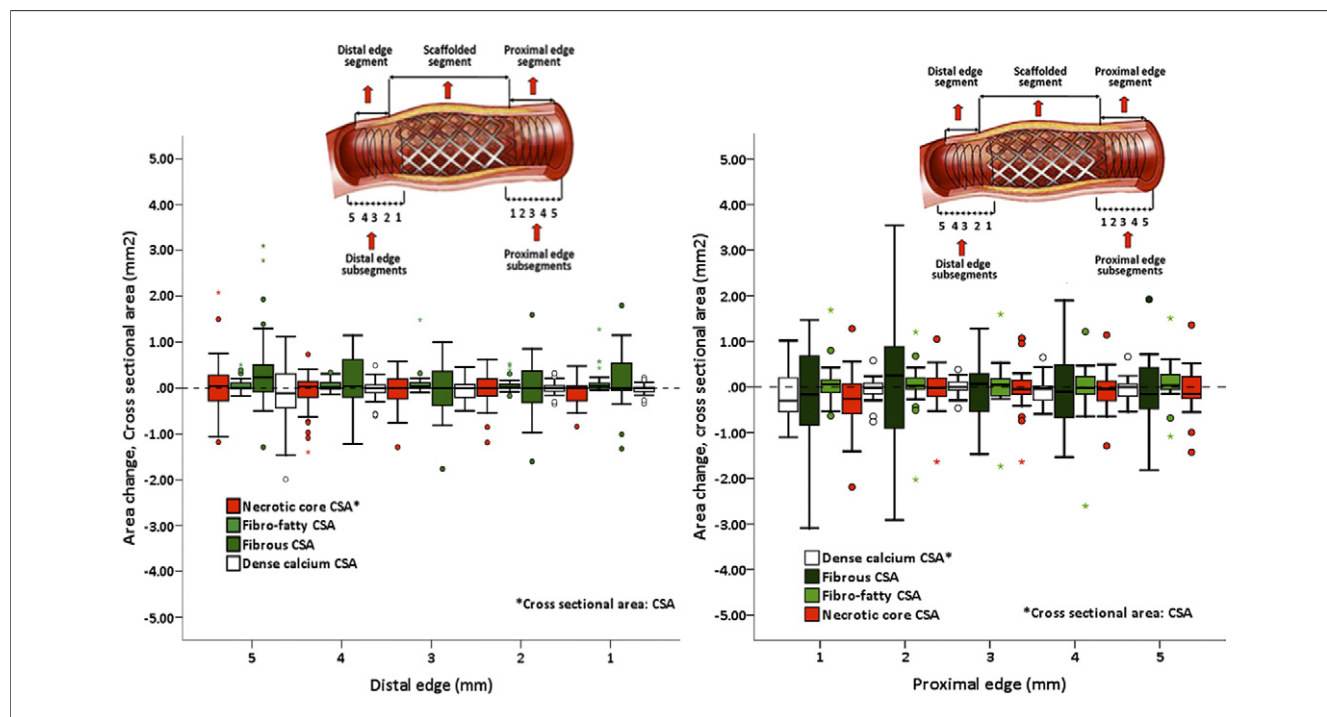
Figure 4. Subsegmental Analysis of the Tissue Composition Changes at the Proximal and Distal Edges After Implantation of the ABSORB BVS

The analysis, per mm of the subsegments, was performed at 1-year follow-up. BVS = bioresorbable vascular scaffold.

conformability (16) of the ABSORB BVS device, proximal constrictive remodeling was observed at 1-year after implantation, and further investigations are required to evaluate the changes of WSS at the scaffold edges or the in-scaffold area. Moreover, any of the initial flow–tissue interaction effects caused by the implantation of this bioresorbable device are expected to potentially subside after a 2-year period when the bioresorption process is expected to be complete and the polymeric platform is fully transformed to CO_2 and H_2O, with no consequent remaining compliance mismatch (8,16). Samady et al. (17) recently demonstrated, in a cohort of 20 patients, that coronary segments with low WSS (step-up regions) are segments that develop constrictive remodeling, in contrast to the high-WSS segments that present excessive expansive remodeling with tissue composition changes, mainly due to an increase in DC and NC tissue components. These reported observations are in parallel with the present findings in this study regarding vessel geometry and tissue composition.

The distal edge segment adjacent to the scaffold appeared to have major tissue composition changes with some degree of plaque progression, which caused a subsequent nonsignificant expansive remodeling. The VH-IVUS–derived tissue type that correlates with extracellular matrix is the FF tissue, which happens to be the one that increased the most (18). The DC tissue component appeared to have a biphasic response at this segment after the ABSORB BVS implan-

tation with a significant increase at 6 months and a trend toward a decrease at 1-year follow-up; conversely, the NC tissue changed nonsignificantly following sequential modifications of DC tissue.

The changes in DC and NC tissue components at follow-up should be interpreted with caution since the ABSORB BVS is made of bioresorbable polymeric material recognized as "pseudo" DC and NC, parameters that have previously been reported as surrogate markers of the bioresorption process (19,20). In addition, the edges of the polymeric scaffold are not sharply demarcated since the vessel surrounding the imaging device are affected by the "to and fro" motion of the cardiac contraction, causing a "pseudoaxial" displacement of the IVUS catheter related to the arterial wall.

Indeed, the cardiac cycle can cause a mean axial displacement of the IVUS transducer of 1.5 mm with a maximum distortion up to 6.5 mm; however, the use of electrocardiogram gating during IVUS data acquisition reduces the axial movement to a maximum of 0.8 mm (21–23) but does not fully prevent the imaging of the polymeric struts as "pseudo" DC in the adjacent edge of the implanted device. In keeping with the standard operational procedure of an independent core laboratory (Cardialysis), the quantification of the scaffold edges was initiated at the point where the visualization of the scaffold arc at each frame was <360°, implying that the scaffold edge to some extent may include polymeric struts.

The apparent increase in DC at 6 months, followed by a trend toward a reduction at 1 year, accompanied by the parallel behavior of the NC, are attributed to the introduction of the bioresorbable device during the procedure and subsequent bioresorption process long term. Other possible factors that may have influenced the NC tissue component are the locally eluted drug everolimus and the systemic use of HMG-CoA inhibitors. Verheye et al. (24) recently demonstrated that everolimus—an inhibitor of the mammalian target of rapamycin (m-TOR)—has autophagic capabilities on macrophages, with a subsequent effect of diminishing NC formation, inflammation, and thrombosis. Hong et al. (25) reported a significant 13% relative reduction in plaque necrotic core volume, and a significant 27% relative increase in plaque FF content with the administration of HMG-CoA inhibitors, assessed with VH-IVUS at 1-year follow-up.

Coronary endothelial dysfunction has been previously associated with underlying plaque composition, in particular high content of DC and NC. Lavi et al. (26) have demonstrated impaired endothelial-dependent vasomotion in vessel segments with underlying NC-rich plaques. Our group has recently demonstrated that the restored normal vasodilatory response to acetylcholine in coronary segments that have previously undergone implantation with an AB-SORB BVS, is associated with a reduction of NC (27), implying the potential restoration of the vasomotor function of the treated vessel with reductions of specific tissue components. Whether the present findings are due to the combined effects of locally eliminated m-TOR inhibitor everolimus, with the systemic use of the HMG-CoA inhibitors, or the natural history of the bioresorbable process of the implanted device, remains to be elucidated in future studies, where a potential restoration of the vasomotor function at the scaffold edges would be highly expected with the sustained tissue composition changes observed at 1-year follow-up. Furthermore, the combination of continuous polymer degradation and elaboration of the treated vessel from its foreign material beyond 1 year, with the restoration of vessel biological behavior (vasomotor function) and the interplay with pharmacological intervention may potentially eliminate the risk of late stent thrombosis.

The clinical outcome of the ABSORB Cohort B trial at 1-year post implantation of the ABSORB BVS revealed a hierarchical major adverse cardiac event rate of 6.9%, with no episodes of scaffold thrombosis (according to the protocol or Academic Research Consortium definitions). Pre-scaffolding VH-IVUS analysis can give an insight into the extent of plaque and NC within and beyond the intended scaffolded segment. This latter point is potentially important, since full coverage of the lesion by the implanted device is the desired goal of the interventionalist, as incomplete coronary plaque coverage has been reported to effect

long-term clinical events, especially in the presence of NC-containing plaques (11).

Study limitations. The main limitation of our study is the small number of the investigated scaffold edges. The complete cohort (B_1+B_2) at the different time points without splitting the population would potentially have increased the sample size; this, however, was a predefined design of the study.

Conclusions

The edge vascular response, with the use of the ABSORB BVS device at 1-year post implantation, demonstrates a degree of proximal edge constrictive remodeling and distal edge plaque compositional changes, a biological behavior similar to that observed with the metallic devices. Full bioresorption of the device, expected to occur in approximately 2 years, will potentially allow for the evaluation and comparison of the exact biological composition of the treated vessel at the scaffold edges, utilizing the VH-IVUS imaging modality.

Reprint requests and correspondence: Prof. P. W. Serruys, Thoraxcenter, Bd583a, Dr. Molewaterplein 40, 3015-GD Rotterdam, the Netherlands. E-mail: p.w.j.c.serruys@erasmusmc.nl.

REFERENCES

1. Costa MA, Angiolillo DJ, Tannenbaum M, et al. Impact of stent deployment procedural factors on long-term effectiveness and safety of sirolimus-eluting stents (final results of the multicenter prospective STLLR trial). Am J Cardiol 2008;101:1704–11.
2. Grube E, Silber S, Hauptmann KE, et al. TAXUS I: six- and twelve-month results from a randomized, double-blind trial on a slow-release paclitaxel-eluting stent for de novo coronary lesions. Circulation 2003;107:38–42.
3. Serruys PW, Degertekin M, Tanabe K, et al. Vascular responses at proximal and distal edges of paclitaxel-eluting stents: serial intravascular ultrasound analysis from the TAXUS II trial. Circulation 2004;109:627–33.
4. García-García HM, Gonzalo N, Tanimoto S, Meliga E, de Jaegere P, Serruys PW. Characterization of edge effects with paclitaxel-eluting stents using serial intravascular ultrasound radiofrequency data analysis: the BETAX (BEside TAXus) study. Rev Esp Cardiol 2008;61:1013–9.
5. Chieffo A, Foglieni C, Nodari RL, et al. Histopathology of clinical coronary restenosis in drug-eluting versus bare metal stents. Am J Cardiol 2009;104:1660–7.
6. Byrne RA, Eberle S, Kastrati A, et al. Distribution of angiographic measures of restenosis after drug-eluting stent implantation. Heart 2009;95:1572–8.
7. Onuma Y, Serruys PW, Perkins LE, et al. Intracoronary optical coherence tomography and histology at 1 month and 2, 3, and 4 years after implantation of everolimus-eluting bioresorbable vascular scaffolds in a porcine coronary artery model: an attempt to decipher the human optical coherence tomography images in the ABSORB trial. Circulation 2010;122:2288–300.
8. Gogas BD, Radu M, Onuma Y, et al. Evaluation with in vivo optical coherence tomography and histology of the vascular effects of the everolimus-eluting bioresorbable vascular scaffold at two years following implantation in a healthy porcine coronary artery model: implications of pilot results for future pre-clinical studies. Int J Cardiovasc Imaging 2012;28:499–516.
9. Gogas BD, Farooq V, Serruys PW, et al. Assessment of coronary atherosclerosis by IVUS and IVUS-based imaging modalities: progres-

sion and regression studies, tissue composition and beyond. Int J Cardiovasc Imaging 2011;27:225–37.

10. Hoffmann R, Guagliumi G, Musumeci G, et al. Vascular response to sirolimus-eluting stents delivered with a nonaggressive implantation technique: comparison of intravascular ultrasound results from the multicenter, randomized e-Sirius, and Sirius trials. Catheter Cardiovasc Interv 2005;66:499–506.

11. Farb A, Burke AP, Kolodgie FD, Virmani R. Pathological mechanisms of fatal late coronary stent thrombosis in humans. Circulation 2003; 108:1701–6.

12. Wentzel JJ, Gijsen FJ, Stergiopulos N, Serruys PW, Slager CJ, Krams R. Shear stress, vascular remodeling and neointimal formation. J Biomech 2003;36:681–8.

13. Wentzel JJ, Whelan DM, van der Giessen WJ, et al. Coronary stent implantation changes 3-d vessel geometry and 3-d shear stress distribution. J Biomech 2000;33:1287–95.

14. Thury A, Wentzel JJ, Vinke RV, et al. Images in cardiovascular medicine. Focal in-stent restenosis near step-up: roles of low and oscillating shear stress? Circulation 2002;105:e185–7.

15. Gomez-Lara J, Garcia-Garcia HM, Onuma Y, et al. A comparison of the conformability of everolimus-eluting bioresorbable vascular scaffolds to metal platform coronary stents. J Am Coll Cardiol Intv 2010;3:1190–8.

16. Tortoriello A, Pedrizzetti G. Flow-tissue interaction with compliance mismatch in a model stented artery. J Biomech 2004;37:1–11.

17. Samady H, Eshtehardi P, McDaniel MC, et al. Coronary artery wall shear stress is associated with progression and transformation of atherosclerotic plaque and arterial remodeling in patients with coronary artery disease. Circulation 2011;124:779–88.

18. Farb A, Kolodgie FD, Hwang JY, et al. Extracellular matrix changes in stented human coronary arteries. Circulation 2004;110:940–7.

19. Kim SW, Mintz GS, Hong YJ, et al. The virtual histology intravascular ultrasound appearance of newly placed drug-eluting stents. Am J Cardiol 2008;102:1182–6.

20. Bruining N, de Winter S, Roelandt JR, et al. Monitoring in vivo absorption of a drug-eluting bioabsorbable stent with intravascular ultrasound-derived parameters a feasibility study. J Am Coll Cardiol Intv 2010;3:449–56.

21. Arbab-Zadeh A, DeMaria AN, Penny WF, Russo RJ, Kimura BJ, Bhargava V. Axial movement of the intravascular ultrasound probe during the cardiac cycle: implications for three-dimensional reconstruction and measurements of coronary dimensions. Am Heart J 1999;138: 865–72.

22. von Birgelen C, de Vrey EA, Mintz GS, et al. ECG-gated three-dimensional intravascular ultrasound: feasibility and reproducibility of the automated analysis of coronary lumen and atherosclerotic plaque dimensions in humans. Circulation 1997;96:2944–52.

23. Bruining N, von Birgelen C, de Feyter PJ, et al. ECG-gated versus nongated three-dimensional intracoronary ultrasound analysis: implications for volumetric measurements. Cathet Cardiovasc Diagn 1998; 43:254–60.

24. Verheye S, Martinet W, Kockx MM, et al. Selective clearance of macrophages in atherosclerotic plaques by autophagy. J Am Coll Cardiol 2007;49:706–15.

25. Hong MK, Park DW, Lee CW, et al. Effects of statin treatments on coronary plaques assessed by volumetric virtual histology intravascular ultrasound analysis. J Am Coll Cardiol Intv 2009;2:679–88.

26. Lavi S, Bae JH, Rihal CS, et al. Segmental coronary endothelial dysfunction in patients with minimal atherosclerosis is associated with necrotic core plaques. Heart 2009;95:1525–30.

27. Brugaletta S, Heo HJ, Garcia-Garcia HM, et al. Endothelial-dependent vasomotion in coronary segment treated by ABSORB everolimus-eluting bioresorbable vascular scaffold system is related to plaque composition at the time of bioresorption of the polymer: indirect finding of vascular reparative therapy? Eur Heart J 2012 Apr 16 [E-pub ahead of print].

Key Words: ABSORB bioresorbable vascular scaffold ■ edge vascular response ■ virtual histology intravascular ultrasound assessment.

▷ **APPENDIX**

For supplemental material, please see the online version of this article.